ELSEVIER

Solid State Sciences 3 (2001) 829–835

Solid State Sciences

www.elsevier.com/locate/ssscie

Syntheses and characterization of $Co(pydc)(H_2O)_2$ and $Ni(pydc)(H_2O)$ (pydc = 3,5-pyridinedicarboxylate)

Tabatha Whitfield, Li-Min Zheng [1], Xiqu Wang, Allan J. Jacobson *

Department of Chemistry, University of Houston, Houston, TX 77204-5641, USA

Received 20 December 2000; accepted 25 September 2001

Abstract

The hydrothermal reaction of 3,5-pyridinedicarboxylic acid ($pydcH_2$) and $Co(NO_3)_2$ or $Ni(NO_3)_2$ in the presence of 4,4′-bipyridine results in two novel compounds $Co(pydc)(H_2O)_2$ (**1**) and $Ni(pydc)(H_2O)$ (**2**). Crystal data: **1**, monoclinic, C2/c, $a = 9.900(2)$, $b = 11.984(2)$, $c = 7.3748(15)$ Å, $\beta = 105.37(3)°$, $V = 843.7(3)$ Å^3, $Z = 4$; **2**, monoclinic, $P2_1/c$, $a = 7.7496(6)$, $b = 15.0496(11)$, $c = 6.4224(5)$ Å, $\beta = 108.437(1)°$, $V = 710.59(9)$ Å^3, $Z = 4$. The structure of **1** is composed of honeycomb layers built up from $\{CoO_4N\}$ trigonal bipyramids and 3,5-pyridinedicarboxylate bridges. The structure of **2** adopts a three-dimensional framework structure in which the Ni atoms are coordinated by the pydc bridges both within the honeycomb layer and between the layers. The magnetic properties of **1** and **2** have been investigated.

Keywords: Coordination polymers; Cobalt; Nickel; Pyridinedicarboxylic acid; Crystal structure; Magnetism

1. Introduction

In recent years, efforts have been made to explore the synthesis of metal-organic compounds with open-framework or microporous structures because of their potential applications in molecular recognition, separation and catalysis [1–14]. Several studies have used rigid, multifunctional ligands to bridge metal ions into two- or three-dimensional structures. Among these ligands, the aromatic carboxylates such as 1,3,5-benzenetricarboxylate (btc) and 1,4-benzenedicarboxylate (bdc) have been used successfully to synthesize such materials [10–14]. However, even when the same multifunctional ligand is used, structures with different dimensionalities can be formed. For example, the compound $[Cu(btcH)(H_2O)_3]_n$ [15] has a chain structure but the compound $[Cu_3(btc)_2(H_2O)_3]_n$ [12] has a three-dimensional microporous structure although both contain the same btc ligand. Factors such as solvent, pH and reaction temperature appear to control the dimensionality though the different coordination chemistries of the metal ions also play an important role in determining the crystal structures of the corresponding metal-organic polymers.

In this paper, we report the crystal structures and characterization of two new compounds: $Co(pydc)(H_2O)_2$ (**1**) and $Ni(pydc)(H_2O)$ (**2**), where pydc represents 3,5-pyridinedicarboxylate. The former has a layer structure whereas the latter is a three-dimensional framework.

2. Experimental

2.1. Materials and methods

All the starting materials were reagent grade and used as purchased. The infrared spectra were recorded on a Galaxy FTIR 5000 series spectrometer with pressed KBr pellets. Thermal analyses were performed in air with a

* Correspondence and reprints.
E-mail address: ajjacob@uh.edu (A.J. Jacobson).
[1] On leave from the State Key Laboratory of Coordination Chemistry, Coordination Chemistry Institute, Nanjing University, Nanjing 210093, PR China.

1293-2558/01/$ – see front matter
PII: S1293-2558(01)01218-3

heating rate of 5 °C min^{-1} on a TGA V5.1A Dupont 2100 instrument. Magnetic susceptibility data were obtained on polycrystalline samples from 2 to 300 K in a magnetic field of 5 kG using a SQUID magnetometer. Diamagnetic corrections were estimated from Pascal's constants [16].

2.2. Synthesis of Co(pydc)(H_2O)$_2$ (1)

The compound was first synthesized by heating a mixture of $Co(NO_3)_2 \bullet 6H_2O$ (0.5 mmol, 0.1464 g), NH_4VO_3 (0.5 mmol, 0.0590 g), 3,5-pyridinedicarboxylic acid (0.5 mmol, 0.0836 g) and H_2O (8 ml) in a Teflon-lined autoclave (23 ml) at 160 °C for 3 d. Red crystals of the title compound appeared as a minor phase, together with large amount of unidentified yellow microcrystallites. A pure phase was obtained by reacting a mixture of $Co(NO_3)_2 \bullet 6H_2O$ (0.5 mmol, 0.1454 g), 3,5-pyridinedicarboxylic acid (0.5 mmol, 0.0845 g), 4,4′-bipyridine (0.5 mmol, 0.0781 g) and H_2O (8 ml) at 160 °C for 5 d. Yield: 72%. IR (KBr, cm^{-1}): 3320br, 1690m, 1615s, 1555s, 1462s, 1441s, 1402s, 1300m, 1240vw, 1208vw, 1152m, 1128m, 1034m, 939m, 853m, 810w, 790s, 754s, 698m, 673m, 590s, 523w, 446w, 426w.

2.3. Synthesis of Ni(pydc)(H_2O) (2)

Hydrothermal reaction of a mixture of $Ni(NO_3)_2 \bullet 6H_2O$ (0.5 mmol, 0.1454 g), 3,5-pyridinedicarboxylic acid (0.5 mmol, 0.0845 g), 4,4′-bipyridine (0.5 mmol, 0.0781 g) and H_2O (8 ml) at 200 °C for 1 d leads to the formation of green plate-like crystals of the compound **2** as a single phase. Yield: 56%. IR (KBr, cm^{-1}): 3523br, 3189br, 3083m, 3056m, 1626s, 1587m, 1542s, 1462s, 1382s, 1301m, 1250w, 1138m, 1030m, 845s, 776m, 739s, 692w, 526w, 439w.

A pure phase of compound **2** can also be obtained by replacing 4,4′-bipyridine by pyrazine.

2.4. Crystallographic studies

Single crystals of dimensions $0.10 \times 0.12 \times 0.08$ mm^3 for **1** and $0.12 \times 0.10 \times 0.04$ mm^3 for **2** were used for structural determinations. All measurements were made with a Siemens SMART platform diffractometer equipped with a 1K CCD area detector. A hemisphere of data (1271 frames at 5 cm detector distance) was collected using a narrow-frame method with scan widths of 0.30° in ω and an exposure time of 35 s $frame^{-1}$ for **1** and 25 s $frame^{-1}$ for **2**. The first 50 frames were re-measured at the end of data collection to monitor instrument and crystal stability, and the maximum correction applied to the intensities was < 1%. The data were integrated using the Siemens SAINT program [17], with the intensities corrected for Lorentz factor, polarization, air absorption, and absorption due to variation in the path length through the detector faceplate. Number of measured, unique and observed reflections [$I > 2\sigma(I)$]: 4663, 992, 953 (R_{int} = 0.0193) for **1**; 3259, 1052, 962 (R_{int} = 0.0165) for **2**. Empirical absorption and the extinction corrections were applied for both compounds.

The structures were solved by direct methods and refined on F^2 by full-matrix least squares using SHELXTL [18]. All non-hydrogen atoms were refined with anisotropic displacement parameters. The hydrogen atoms were refined isotropically. Crystallographic data of the two compounds are summarized in Table 1, atom positions in Tables 2, 4 and selected bond lengths and angles in Tables 3, 5.

3. Results and discussion

3.1. Structure descriptions

Compound **1** crystallizes in space group C2/c. Fig. 1 shows the building unit of **1** with the atomic labeling scheme. The Co(1) atom has a distorted trigonal bipyramidal geometry. The three equatorial positions are occupied by the O(1), O(1A) and N(1B) atoms from three equivalent pydc groups. The sum of bond angles in the basal plane is 360°. Two water molecules occupy the two axial positions. The Co–O (2.077(2), 2.155(2) Å) and Co–N (2.193(3) Å) bond distances are as expected. The pydc ligand is tri-dentate and bridges three equivalent cobalt atoms. The O(2) atom of each carboxylate group is terminal and oriented to the Co(1) atom with the Co(1)...O(2) distance 2.433 Å. A two-dimensional layer structure is thus constructed in the *ab*-plane with openings along the *c*-direction (Fig. 2). Hydrogen bonds are formed between coordinated water molecules and the carboxylate oxygens of adjacent layers. (O(1w)···O(1) 2.786 Å, O(1w)···O(2) 2.761 Å) (Fig. 3). The shortest Co···Co distance within the layer is 7.772 Å, and that between the layers is 5.347 Å.

Compound **2** crystallizes in space group $P2_1/c$ with a three-dimensional framework structure, significantly different from that of **1**. In contrast to the Co atom environment in **1**, the Ni atom has distorted octahedral geometry with the equatorial positions occupied by three carboxylate O atoms and one pyridine N atom (Fig. 4). The

Table 1
Crystallographic data

Compound	**1**	**2**
Formula	$C_7H_7CoNO_6$	$C_7H_5NNiO_5$
M	260.07	241.83
Crystal system	Monoclinic	Monoclinic
Space group	C2/c	$P2_1/c$
a (Å)	9.900(2)	7.7496(6)
b (Å)	11.984(2)	15.050(1)
c (Å)	7.375(2)	6.4224(5)
β (deg)	105.37(3)	108.437(1)
V (Å^3)	843.7(3)	710.59(9)
Z	4	4
D_c (g cm^{-3})	2.047	2.260
$F(000)$	524	488
μ (Mo $K\alpha$) (cm^{-1})	20.43	27.22
Goodness of fit on F^2	1.151	1.052
R_1, wR_2[a] $[I > 2\sigma(I)]$	0.0205, 0.0561	0.0209, 0.0547
R_1, wR_2 (all data)	0.0214, 0.0565	0.0231, 0.0554
Extinction coefficient	0.0145(14)	0.0031(7)
$(\Delta\rho)_{max}$, $(\Delta\rho)_{min}$ (e Å^{-3})	0.458, −0.381	0.321, −0.250

[a] $R_1 = \sum \|F_o| - |F_c\| / \sum |F_o|$, $wR_2 = [\sum w(F_o^2 - F_c^2)^2 / \sum w(F_o^2)^2]^{1/2}$.

Table 2
Atomic coordinates and equivalent isotropic displacement parameters (Å^2) for **1**

Atom	x	y	z	U_{iso} (Å^2)
Co1	0.5000	0.16157(2)	0.2500	0.0103(1)
N1	0.0000	−0.15547(13)	0.2500	0.0116(3)
O1	0.36280(11)	0.02323(9)	0.25943(16)	0.0181(2)
O2	0.24847(12)	0.18102(9)	0.20031(17)	0.0198(2)
O1W	0.53741(13)	0.17035(9)	0.54045(16)	0.0167(2)
C1	0.11242(14)	−0.09723(12)	0.2336(2)	0.0119(3)
H1A	0.1899	−0.1364	0.2187	0.014
C2	0.11824(13)	0.01891(11)	0.23799(19)	0.0113(3)
C3	0.0000	0.07788(16)	0.2500	0.0120(4)
H3A	0.0000	0.1555	0.2500	0.014
C4	0.25066(14)	0.07813(12)	0.23150(19)	0.0122(3)
H2A	0.556(2)	0.114(2)	0.589(3)	0.033(6)
H2B	0.595(2)	0.214(2)	0.583(3)	0.025(5)

Table 3
Selected bond lengths (Å) and angles (deg) for **1**

Co(1)–O(1W)	2.078(1) × 2
Co(1)–N(1[b])	2.193(2)
O(1)–C(4)	1.260(2)
C(1)–C(2)	1.393(2)
C(2)–C(4)	1.503(2)
Co(1)–O(1)	2.156(1) × 2
N(1)–C(1)	1.346(2)
O(2)–C(4)	1.253(2)
C(2)–C(3)	1.390(2)
O(1WA)–Co(1)–O(1W)	174.20(6)
O(1W)–Co(1)–O(1)	86.98(5) × 2
O(1W)–Co(1)–N(1[b])	87.10(3) × 2
C(1C)–N(1)–C(1)	117.5(2)
C(4)–O(1)–Co(1)	97.4(1)
C(1)–C(2)–C(3)	118.6(1)
C(3)–C(2)–C(4)	121.2(1)
O(2)–C(4)–O(1)	121.0(1)
O(1)–C(4)–C(2)	119.1(1)
O(1W[a])–Co(1)–O(1)	97.5(1) × 2
O(1)–Co(1)–O(1[a])	79.5(1)
O(1)–Co(1)–N(1[b])	140.3(1) × 2
C(1[c])–N(1)–Co(1[d])	121.2(1)
N(1)–C(1)–C(2)	123.1(1)
C(1)–C(2)–C(4)	120.2(1)
C(2C)–C(3)–C(2)	118.9(2)
O(2)–C(4)–C(2)	119.9(1)

Symmetry transformations used to generate equivalent atoms:
[a] $-x+1, y, -z+1/2$; [b] $x+1/2, y+1/2, z$; [c] $-x, y, -z+1/2$; [d] $x-1/2, y-1/2, z$.

axial positions are occupied by one carboxylate oxygen atom and one water molecule. The Ni–O and Ni–N bond lengths are 2.005(2)–2.141(2) Å and 2.064(2) Å, respectively. The atoms that occupy the equatorial positions of each Ni octahedron are from three equivalent pydc ligands. Each pydc ligand bridges three equivalent Ni centers to give a two-dimensional layer of $\{Ni(pydc)\}_n$ in the *ab*-plane (Fig. 5). The layers in **1** and **2** are related but in **2**, the 3,5-pyridinedicarboxylate ligand acts as a pentadentate ligand, whereas in **1** it is tridentate. One carboxylate in **2** is chelated to the metal center (O(3B)–Ni–O(4B) 61.85(7)°).

The second carboxylate group coordinates the Ni^{2+} through a single O atom in the *ab*-plane and the other

Table 4
Atomic coordinates and equivalent isotropic displacement parameters ($Å^2$) for **2**

Atom	x	y	z	U_{iso} ($Å^2$)
Ni1	0.72476(4)	0.41704(2)	0.24885(5)	0.0150(2)
N1	0.5062(3)	0.34612(13)	0.2798(3)	0.0145(5)
O1	0.6054(2)	0.07696(11)	0.4040(3)	0.0209(4)
O2	0.3152(2)	0.04716(12)	0.2171(3)	0.0213(4)
O3	−0.0157(2)	0.43926(11)	0.2164(3)	0.0207(4)
O4	−0.1162(2)	0.30383(11)	0.2223(3)	0.0200(4)
O1W	0.8442(3)	0.41180(12)	0.5904(3)	0.0241(4)
H1WA	0.8950(39)	0.4614(12)	0.6555(44)	0.029
H1WB	0.7764(34)	0.4026(20)	0.6761(41)	0.029
C1	0.5357(3)	0.2581(2)	0.3047(4)	0.0150(5)
H1	0.6621(39)	0.2394(18)	0.3338(42)	0.022
C2	0.3978(3)	0.1971(2)	0.2826(4)	0.0135(5)
C3	0.2223(3)	0.2283(2)	0.2436(4)	0.0135(5)
H3	0.1313(39)	0.1931(19)	0.2301(45)	0.020
C4	0.1916(3)	0.3194(2)	0.2336(4)	0.0135(5)
C5	0.3367(3)	0.3757(2)	0.2473(4)	0.0140(5)
H5	0.3176(39)	0.4325(20)	0.2285(43)	0.021
C6	0.4430(3)	0.0991(2)	0.3036(4)	0.0138(5)
C7	0.0093(3)	0.3558(2)	0.2207(4)	0.0151(6)

oxygen atom bridges two Ni atoms from adjacent {Ni(pydc)}$_n$ layers, to form a three-dimensional framework (Fig. 6). The Ni(OCO)$_2$Ni dimers that are present between adjacent layers allow for an efficient magnetic interaction between the Ni centers propagated through the carboxylate bridges. The Ni···Ni distance within the dimer is 4.642 Å while the shortest Ni···Ni distance within the layer is 5.966 Å through the pydc bridge. Hydrogen bonds are also found between the layers (O(1w)···O(3) 2.700 Å).

The difference between the structures of **1** and **2** originates from the different coordination modes of Co^{2+} and Ni^{2+} ions in that Ni^{2+} has a stronger preference for octahedral geometry whereas Co^{2+} can adopt a variety of geometries when coordinated by weak field ligands. For example, in the compound $NaCo_3(OH)(PO_4)_2 \bullet 1/4H_2O$ three distinct cobalt sites are present with tetrahedral, trigonal bipyramidal, and octahedral coordination [19].

Table 5
Selected bond lengths (Å) and angles (deg) for **2**

Ni(1)–O(2^a)	2.005(2)
Ni(1)–O(1W)	2.095(2)
Ni(1)–O(1^c)	2.115(2)
N(1)–C(5)	1.339(3)
O(1)–C(6)	1.264(3)
O(3)–C(7)	1.270(3)
C(1)–C(2)	1.381(4)
C(2)–C(6)	1.513(3)
C(4)–C(5)	1.389(4)
N(1)–C(5)	1.339(3)
O(1)–C(6)	1.264(3)
O(3)–C(7)	1.270(3)
C(1)–C(2)	1.381(4)
C(2)–C(6)	1.513(3)
C(4)–C(5)	1.389(4)
Ni(1)–N(1)	2.064(2)
Ni(1)–O(3^b)	2.113(2)
Ni(1)–O(4^b)	2.141(2)
N(1)–C(1)	1.345(3)
O(2)–C(6)	1.246(3)
O(4)–C(7)	1.250(3)
C(2)–C(3)	1.385(4)
C(3)–C(4)	1.389(4)
C(4)–C(7)	1.493(3)
N(1)–C(1)	1.345(3)
O(2)–C(6)	1.246(3)
O(4)–C(7)	1.250(3)
C(2)–C(3)	1.385(4)
C(3)–C(4)	1.389(4)
C(4)–C(7)	1.493(3)
O(2^a)–Ni(1)–N(1)	109.55(8)
N(1)–Ni(1)–O(1W)	89.09(8)
N(1)–Ni(1)–O(3^b)	157.97(8)
O(2^a)–Ni(1)–O(1^c)	92.35(7)
O(1W)–Ni(1)–O(1^c)	179.60(7)
O(2^a)–Ni(1)–O(4^b)	153.95(7)
O(1W)–Ni(1)–O(4^b)	88.78(7)
O(1^c)–Ni(1)–O(4^b)	91.29(7)
C(1)–N(1)–Ni(1)	114.0(2)
C(6)–O(2)–Ni(1^e)	133.8(2)
C(7)–O(4)–Ni(1^f)	88.4(1)
O(3)–C(7)–Ni(1^f)	59.6(1)
O(2^a)–Ni(1)–O(1W)	87.42(7)

Table 5 (Continued)

O(2[a])–Ni(1)–O(3[b])	92.34(7)
O(1W)–Ni(1)–O(3[b])	89.43(8)
N(1)–Ni(1)–O(1[c])	91.29(7)
O(3[b])–Ni(1)–O(1[c])	90.26(7)
N(1)–Ni(1)–O(4[b])	96.14(7)
O(3[b])–Ni(1)–O(4[b])	61.85(7)
C(5)–N(1)–Ni(1)	127.4(2)
C(6)–O(1)–Ni(1[d])	123.9(2)
C(7)–O(3)–Ni(1[f])	89.1(1)
O(4)–C(7)–Ni(1[f])	60.9(1)
C(4)–C(7)–Ni(1[f])	173.0(2)

Symmetry transformations used to generate equivalent atoms:
[a] $-x+1, y+1/2, -z+1/2$; [b] $x+1, y, z$; [c] $x, -y+1/2, z-1/2$;
[d] $x, -y+1/2, z+1/2$; [e] $-x+1, y-1/2, -z+1/2$; [f] $x-1, y, z$.

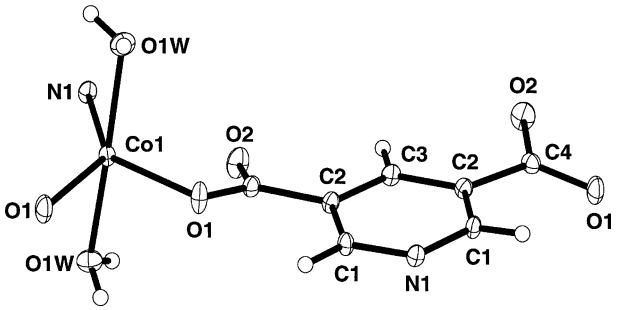

Fig. 1. A fragment of the Co(pydc)(H_2O)$_2$ **1** structure with the atomic labeling scheme (thermal ellipsoids are shown at 50% probability).

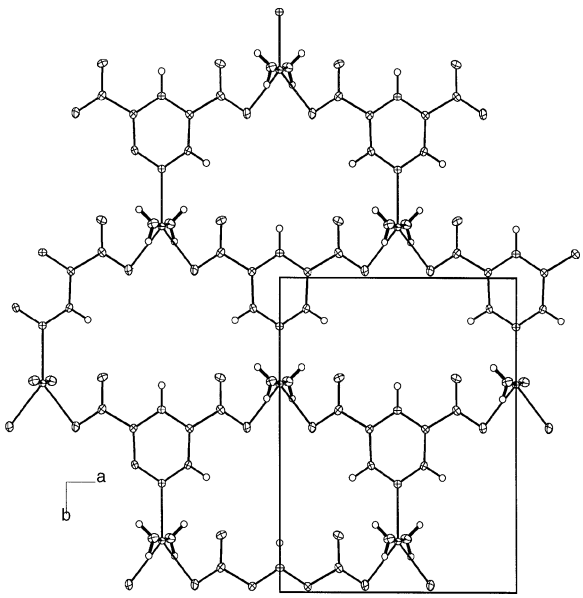

Fig. 2. One layer of the structure of **1** in the *ab*-plane.

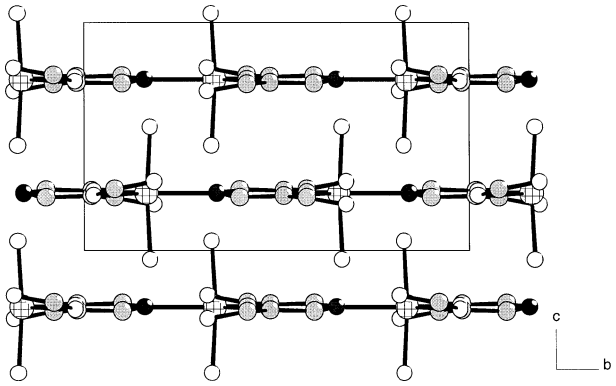

Fig. 3. Packing of the layers in the structure of **1** viewed along [1 0 0].

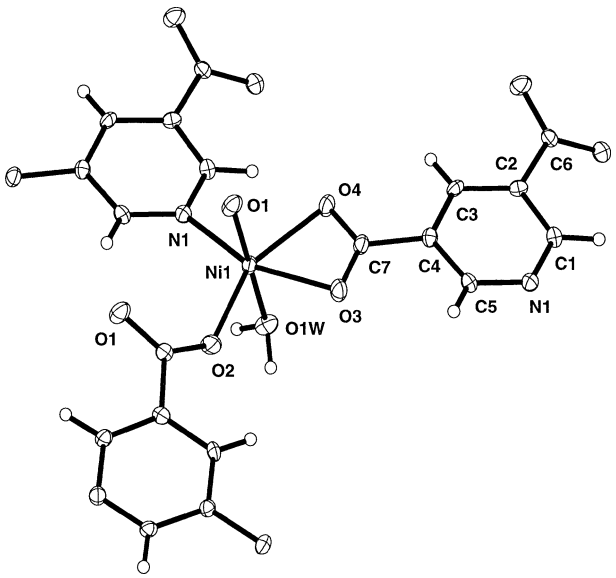

Fig. 4. A fragment of the Ni(pydc)(H_2O) **2** in structure with the atomic labeling scheme (thermal ellipsoids are shown at 50% probability).

3.2. Magnetic properties

The temperature dependent magnetic susceptibilities of **1** and **2** have been studied in the range 2 to 300 K. For **1**, the magnetic moment (μ_{eff}) per cobalt(II) at 300 K is 4.82μ_B, higher than the expected value for the spin-only $S = 3/2$ system (3.87μ_B) due to the orbital contribution. Between 300 and 50 K, the data follow the Curie–Weiss law, leading to the parameters $g = 2.48$, $\theta = +2.75$ K (Fig. 7). The positive θ value suggests a weak ferromagnetic interaction between the Co(II) centers, which is confirmed by the continuous increase of $\chi_m T$ upon cooling to about 50 K. The very weak

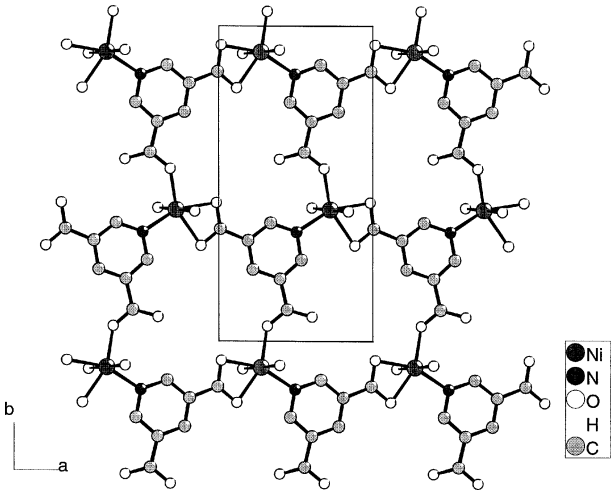

Fig. 5. One layer of the structure of **2** in the *ab*-plane. All H atoms are omitted for clarity.

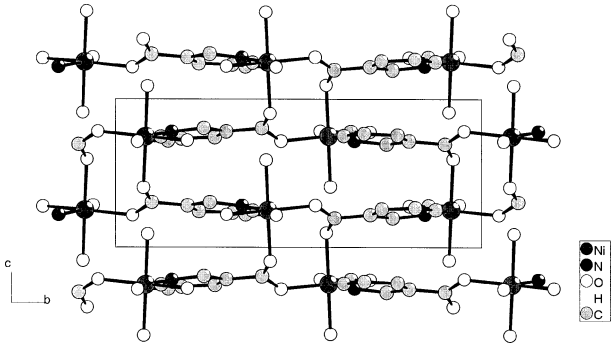

Fig. 6. Packing of the structure of **2** viewed along [1 0 0].

ferromagnetic interaction may be propagated through the pydc bridge within the $\{Co(pydc)\}_n$ layer or through the strong hydrogen bonds between the layers. A theoretical fit based on the isotropic dimer or chain model, however, was not successful.

The magnetic behavior of **2** is shown in Fig. 8 in the forms of χ_m and $\chi_m T$ vs. T. At 300 K, the magnetic moment per Ni(II) ($3.14\mu_B$) is close to the expected spin-only value for $S = 1$ ion ($2.97\mu_B$ for $g = 2.1$). Upon cooling from room temperature, the $\chi_m T$ value increases continuously from 1.233 $cm^3\,K\,mol^{-1}$ at 300 K to a maximum of 1.292 $cm^3\,K\,mol^{-1}$ at 18 K. This behavior is characteristic of a ferromagnetic coupling between the Ni(II) ions. Further cooling below 18 K causes the $\chi_m T$ to decrease, reaching a value of 0.273 $cm^3\,K\,mol^{-1}$ at 2 K.

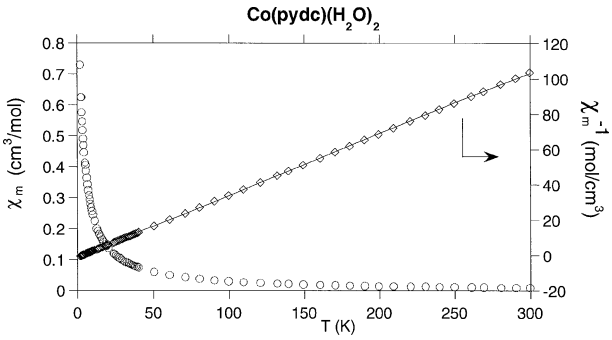

Fig. 7. χ_m and χ_m^{-1} vs. T plots for **1**.

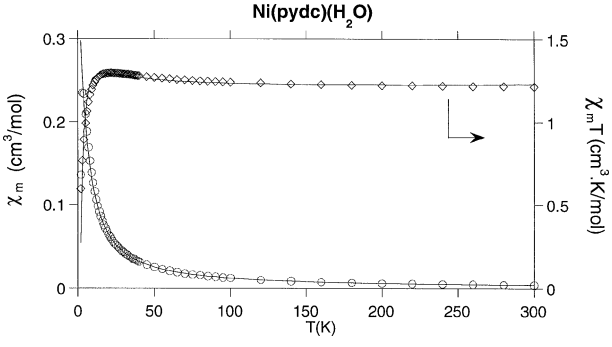

Fig. 8. χ_m and $\chi_m T$ vs. T plots for **2**.

In the structure of compound **2**, the Ni(II) ions are bridged by pydc ligands forming $\{Ni(pydc)\}_n$ layers in the *ab*-plane. The shortest Ni...Ni distance within this layer is 5.966 Å across the pydc ligand. Between the layers, the Ni(II) ions are further linked by the carboxylate oxygens from the neighboring layer which results in the formation of carboxylate bridged $Ni(OCO)_2Ni$ dimers. The Ni···Ni distance within this dimer is 4.642 Å, much shorter than that across the pydc bridge. The super-exchange coupling within the dimer should be dominant. The magnetic behavior below 18 K could be due to the zero-field splitting of the ground state and/or the inter-dimer interaction. The susceptibility data were thus analyzed using the Heisenberg Hamiltonian:

$$\widehat{H} = -2J\widehat{S}_1 \cdot \widehat{S}_2 - \beta\left(g_1\widehat{S}_1 + g_2\widehat{S}_2\right) \cdot \vec{H},$$

with the theoretical equation [20,21]:

$$\chi_m = \frac{Ng^2\beta^2F(J,T)}{kT - 4z'J'F(J,T)},$$

$$F(J,T) = \frac{5 + \exp(-4J/kT)}{5 + 3\exp(-4J/kT) + \exp(-6J/kT)},$$

where N, g, β have their usual meanings, J is the coupling constant between the nickel ions, $z'J'$ accounts for the inter-dimer interaction. A good fit was obtained, shown as the solid line in Fig. 8, with $g = 2.19$, $J = 3.25\ \mathrm{cm}^{-1}$, $z'J' = -0.70\ \mathrm{cm}^{-1}$.

It has been found that weak ferromagnetic interactions are propagated in the carboxylate-bridged copper(II) compounds in which the carboxylate adopts the *anti-syn* conformation and the Cu–O–C–O–Cu skeleton deviates from planarity [22,23]. This result demonstrates that the same phenomenon is also observed in the Ni compounds.

Acknowledgements

We thank the National Science Foundation (DMR-9805881) and the R.A. Welch Foundation for financial support. This work made use of MRSEC/TCSUH Shared Experimental Facilities supported by the National Science Foundation under Award number DMR-9632667 and the Texas Center for Superconductivity at the University of Houston.

References

[1] J. Janiak, Angew. Chem., Int. Ed. Engl. 36 (1997) 1431.
[2] G.B. Gardner, D. Venkataraman, J.S. Moore, S. Lee, Nature 374 (1995) 792;
Y.-H. Kiang, G.B. Gardner, S. Lee, Z. Xu, E.B. Lobkovsky, J. Am. Chem. Soc. 121 (1999) 8204.
[3] T.J. Barton, L.M. Bull, W.G. Klemperer, D.A. Loy, B. McEnaney, M. Misono, P.A. Monson, G. Pez, G.W. Scherer, J.C. Vartuli, O.M. Yaghi, Chem. Mater. 11 (1999) 2633.
[4] P.J. Hagrman, D. Hagrman, J. Zubieta, Angew. Chem., Int. Ed. Engl. 38 (1999) 2638.
[5] S.R. Batten, R. Robson, Angew. Chem., Int. Ed. Engl. 37 (1998) 1460.
[6] D.M.L. Goodgame, D.A. Grachrogel, D.J. Williams, Angew. Chem., Int. Ed. Engl. 38 (1999) 153.
[7] M. Kondo, T. Okubo, A. Asami, S.-I. Noro, T. Yoshitomi, S. Kitagawa, T. Ishii, H. Matsuzaka, K. Seki, Angew. Chem., Int. Ed. Engl. 38 (1999) 140.
[8] J.S. Seo, D. Whang, H. Lee, S.I. Jun, J. Oh, Y.J. Jeon, K. Kim, Nature 404 (2000) 982.
[9] Y. Diskin-Posner, S. Dahal, I. Goldberg, Angew. Chem., Int. Ed. Engl. 39 (2000) 1288.
[10] (a) O.M. Yaghi, G. Li, H. Li, Nature 378 (1995) 703;
(b) O.M. Yaghi, C.E. Davis, G. Li, H. Li, J. Am. Chem. Soc. 119 (1997) 2861;
(c) H. Li, C.E. Davis, T.L. Groy, D.G. Kelley, O.M. Yaghi, J. Am. Chem. Soc. 120 (1998) 2186;
(d) T.M. Reineke, M. Eddaoudi, M. Fehr, D. Kelley, O.M. Yaghi, J. Am. Chem. Soc. 121 (1999) 1651;
(e) T.M. Reineke, M. Eddaoudi, M. O'Keeffe, O.M. Yaghi, Angew. Chem., Int. Ed. Engl. 38 (1999) 2590.
[11] H.J. Choi, T.S. Lee, M.P. Suh, Angew. Chem., Int. Ed. Engl. 38 (1999) 1405.
[12] S.S.-Y. Chui, S.M.-F. Lo, J.P.H. Charmant, A.G. Orpen, I.D. Williams, Science 283 (1999) 1148.
[13] C.J. Kepert, T.J. Prior, M.J. Rosseinsky, J. Am. Chem. Soc. 122 (2000) 5158.
[14] S.O.H. Gutschke, A.M.Z. Slawin, P.T. Wood, Chem. Commun. (1996) 823.
[15] R. Pech, J. Pickardt, Acta Crystallogr., Sect. C 44 (1988) 992.
[16] O. Kahn, Molecular Magnetism, VCH Publishers Inc., New York, 1993.
[17] SAINT, Program for Data Extraction and Reduction, Siemens Analytical X-ray Instruments Inc., Madison, WI, 1994–1996.
[18] G.M. Sheldrick, SHELXTL, Program for Refinement of Crystal Structures, Siemens Analytical X-ray Instruments Inc., Madison, WI, 1994.
[19] R.P. Bontchev, M.N. Iliev, L.M. Dezaneti, A.J. Jacobson, Solid State Sci., in press.
[20] P. Ginsberg, R.L. Martin, R.W. Brookes, R.C. Sherwood, Inorg. Chem. 11 (1972) 2884.
[21] L.-M. Zheng, J.-S. Zhao, K.-H. Lii, L.-Y. Zhang, Y. Liu, X.-Q. Xin, J. Chem. Soc., Dalton Trans. (1999) 939.
[22] C. Ruiz-Pérez, J. Sanchiz, M.H. Molina, F. Lloret, M. Julve, Inorg. Chem. 39 (2000) 1363.
[23] E. Colacio, M. Ghazi, R. Kivekäs, J.M. Moreno, Inorg. Chem. 39 (2000) 2882.